ACADEMIC PRESS

Available online at www.sciencedirect.com

SCIENCE DIRECT®

Journal of Sound and Vibration 264 (2003) 751–773

JOURNAL OF SOUND AND VIBRATION

www.elsevier.com/locate/jsvi

Passive control of discrete-frequency tones generated by coupled detuned cascades

S. Sawyer[a], S. Fleeter[b,*]

[a] *Department of Mechanical Engineering, University of Akron, Akron, OH 44325, USA*

[b] *School of Mechanical Engineering, Purdue University, 1288 Mechanical Engineering Building, West Lafayette, IN 47907, USA*

Received 16 January 2001; accepted 4 June 2002

Abstract

Discrete-frequency tones generated by rotor–stator interactions are of particular concern in the design of fans and compressors. Classical theory considers an isolated flat-plate cascade of identical uniformly spaced airfoils. The current analysis extends this tuned isolated cascade theory to consider coupled aerodynamically detuned cascades where aerodynamic detuning is accomplished by changing the chord of alternate rotor blades and stator vanes. In a coupled cascade analysis, the configuration of the rotor influences the downstream acoustic response of the stator, and the stator configuration influences the upstream acoustic response of the rotor. This coupled detuned cascade unsteady aerodynamic model is first applied to a baseline tuned stage. This baseline stage is then aerodynamically detuned by replacing alternate rotor blades and stator vanes with decreased chord airfoils. The nominal aerodynamically detuned stage configuration is then optimized, with the stage acoustic response decreased 13 dB upstream and 1 dB downstream at the design operating condition. A reduction in the acoustic response of the optimized aerodynamically detuned stage is then demonstrated over a range of operating conditions.

1. Introduction

The primary noise sources for a high bypass turbofan engine are the fan, the low-pressure or booster compressor, and the low-pressure turbine [1,2]. Their noise signatures include a broadband noise level with large spikes or tones at multiples of the blade passing frequency. For subsonic fans, the acoustic spectrum discrete tones are usually 10–15 dB above the broadband

*Corresponding author. Tel.: +1-765-494-5622; fax: +1-765-494-0539.
E-mail address: fleeter@ecn.purdue.edu (S. Fleeter).

0022-460X/03/$ - see front matter
doi:10.1016/S0022-460X(02)01214-2

level. These discrete tones are generated by periodic blade row unsteady aerodynamic interactions between adjacent airfoil rows. Namely, turbomachine airfoil rows are subject to spatially non-uniform inlet flow fields resulting from either potential or viscous wake interactions. Both of these interactions result in the generation of acoustic waves that may propagate unattenuated and interact with other airfoil rows. In this way, the airfoil rows of the turbomachine are coupled, i.e., the response of an airfoil row acts as an excitation to neighboring airfoil rows.

Cascade coupling has been investigated for conventional uniformly spaced or tuned cascades. Hanson [3] studied mode trapping to explain stage acoustic response. Buffum [4] used similar techniques to determine the influence of coupling on the aeroelastic stability of a one and one-half stage compressor. Silkowski and Hall [5] used mode-coupling techniques to determine the influence of neighboring blade rows on the aerodynamic damping of a multistage turbomachine.

Aerodynamic detuning is defined by designed airfoil-to-airfoil differences of an airfoil row. Thus, aerodynamic detuning influences the airfoil-to-airfoil unsteady aerodynamics of the row. These differences affect the fundamental driving force of discrete-frequency noise generation, the unsteady airfoil surface pressures. Due to aerodynamic detuning, the airfoils do not respond in a classical travelling wave mode typical of a conventional uniformly spaced tuned airfoil row. Aerodynamic detuning is beneficial in aeroelastic problems of flutter and forced response. Analytical and computational studies of cascades operating in both incompressible [6] and compressible flow fields [7] have shown that aerodynamic detuning is beneficial to flutter stability.

Depending on the method of construction, some increased manufacturing cost would be expected given the more complex detuned cascade geometries. For cascades that are constructed as an integrally bladed disk, it is expected that minimal additional cost would be incurred. However cascades constructed using standard fir-tree or other similar methods, additional expense would be expected due to increased inventory requirements.

Aerodynamic detuning is attractive because it is a passive control methodology that does not destroy the dynamic balance of the rotor. An aerodynamically detuned cascade is the superposition of two tuned cascades. Each ideally would be perfectly balanced. After all most centrifugal compressors use short-chord splitter blades without detriment to the mechanical integrity of the compressor.

In this paper, a mathematical model is developed to analyze the unsteady aerodynamics of coupled aerodynamically detuned thin airfoil cascades in a compressible subsonic flow with small unsteady perturbations superimposed. The linearized two-dimensional continuity and momentum equations for inviscid isentropic compressible flow are solved using wave theory, a technique first utilized for a uniformly spaced airfoil cascade. This technique is extended herein to analyze aerodynamically detuned airfoil cascades made up of alternate non-uniformly spaced airfoils with different chord lengths, elastic axis locations and chordwise offset positions. The detuned cascade is constructed by the superposition of two uniformly spaced or conventional tuned cascades. The solution of the governing equations yields the airfoil unsteady bound vortex distribution that is equivalent to the airfoil unsteady pressure distribution. The acoustic response of the detuned cascade is then determined through the superposition of the acoustic response of the constituent cascades. Scattering equations are developed that relate the coupling of neighboring blade rows through the combined excitation and response of the cascades. The effects of coupling and aerodynamic detuning on discrete-frequency noise generation are then demonstrated.

2. Detuned cascade unsteady aerodynamics

To analyze the unsteady aerodynamics of coupled aerodynamically detuned cascades, it is necessary to develop an understanding of the fundamentals of two-dimensional subsonic compressible inviscid flow as applied to a detuned cascade [8]. This detuned cascade analysis is then extended to coupled detuned cascades.

An aerodynamically detuned cascade is depicted in Fig. 1. It is the combination of two uniformly spaced cascades, denoted as Cascade A and B for convenience and identified by indices A and B. The freestream velocity $\vec{W}$ has axial and tangential components $\vec{U}$ and $\vec{V}$. The cascades have the same stagger angle γ and circumferential spacing S. The axial and tangential directions specify the co-ordinate systems (x, y) and (x', y') for Cascades A and B, respectively. The (x, y) and (x', y') co-ordinate systems are identical except that the origin for each co-ordinate system is the leading edge of the reference airfoil of the respective cascade. The chordwise co-ordinate z or z' is in the chordwise or flow direction and is not orthogonal to either the axial or tangential direction. The relationship between the co-ordinate systems is given by $(x, y) = (x' + os\cos\gamma, y' + S_o + os\sin\gamma)$, where os is the chordwise offset of Cascade B and S_o is the tangential distance between the cascades. The airfoils of the constituent cascades may have different lengths where the relative chord is given by chord ratio $C_r = C_B/C_A$. The relative pitch spacing gives the spacing ratio $S_r = S_o/S$. A tuned cascade thus corresponds to a detuned cascade when $S_{detuned} = S = 2S_{tuned}$, $S_r = 0.5$, $C_r = 1.0$, $os = 0.0$.

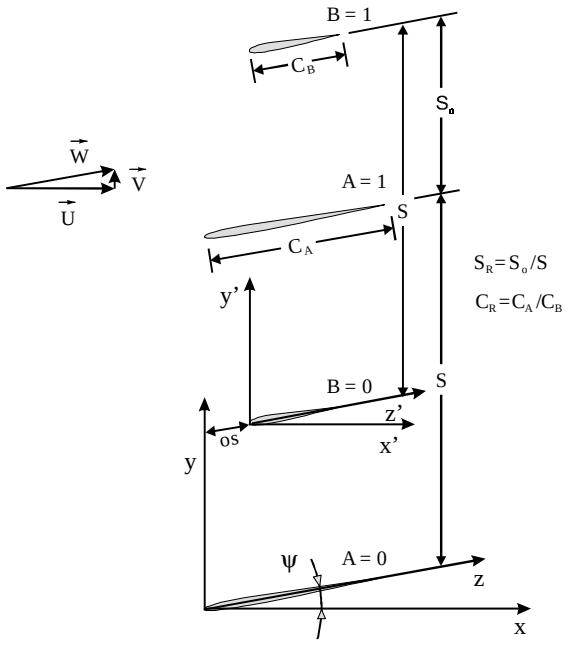

Fig. 1. Detuned cascade geometry.

3. Plane wave solutions of the linearized Euler equations

The two-dimensional inviscid compressible flow continuity and momentum equations linearized about a uniform mean flow are given by

$$\frac{\partial \rho}{\partial t} + U\frac{\partial \rho}{\partial x} + V\frac{\partial \rho}{\partial y} + \rho_\infty\left(\frac{\partial u}{\partial x} + \frac{\partial v}{\partial y}\right) = 0,$$

$$\frac{\partial u}{\partial t} + U\frac{\partial u}{\partial x} + V\frac{\partial u}{\partial y} + \frac{1}{\rho_\infty}\frac{\partial p}{\partial x} = 0,$$

$$\frac{\partial v}{\partial t} + U\frac{\partial v}{\partial x} + V\frac{\partial v}{\partial y} + \frac{1}{\rho_\infty}\frac{\partial p}{\partial y} = 0,$$

where U and V are the steady axial and tangential freestream velocities, u and v are the corresponding unsteady perturbation velocity components, ρ_∞ and ρ are the freestream and perturbation densities and the perturbation pressure is p.

The plane wave solutions are harmonic in time and periodic in x and y.

$$\begin{bmatrix} u \\ v \\ p \end{bmatrix} = \begin{bmatrix} \bar{u} \\ \bar{v} \\ \bar{p} \end{bmatrix} e^{i(\omega t + \alpha x + \beta y)}$$

where $\bar{u}$, $\bar{v}$ and $\bar{p}$ are complex constants specifying the magnitude of the perturbations in pressure and velocity, α and β are the axial and tangential wave numbers and ω is the frequency.

Two families of solutions exist that describe a downstream-convected vorticity wave and upstream and downstream going pressure waves. The first solution family describes a vorticity wave that is simply convected with the mean flow, and has no associated pressure perturbation. The axial wave number for this vorticity wave solution is $\alpha_3 = -(\omega + V\beta)/U$, with vortical gust solutions given subscript 3. The second solution family describes a pair of upstream and downstream going irrotational pressure or acoustic waves. The axial wave numbers for these pressure waves are

$$\alpha_{1,2} = \left[U(\omega + V\beta) \pm a\sqrt{(\omega + V\beta)^2 - (a^2 - U^2)\beta^2}\right] / \left(a^2 - U^2\right)$$

where subscripts 1 and 2 are used to describe upstream and downstream going waves, respectively.

The propagation of the unsteady pressure perturbations or acoustic waves is described by the values of the axial wave number α and depends on the values of the arguments under the radical. For $(\omega + V\beta)^2 - \left(a^2 - U^2\right)\beta^2 > 0$, two real wave numbers exist that describe a pair of acoustic waves that propagate away from the cascade unattenuated. For $(\omega + V\beta)^2 - \left(a^2 - U^2\right)\beta^2 < 0$, complex wave numbers describe acoustic waves that decay exponentially away from the cascade. If $(\omega + V\beta)^2 - \left(a^2 - U^2\right)\beta^2 = 0$, the cascade is in an acoustic resonance condition.

The airfoil cascade unsteady aerodynamic loading is modelled by replacing the airfoils with bound vortex sheets. The bound vortex distribution is then expanded in a Fourier series in the tangential direction, with the harmonics specified by the cascade mode index v. Unsteady cascade

periodicity requirements then specify the tangential wave number β:

$$\beta = \frac{\sigma + 2\pi v}{S}, \quad v = 0, \pm 1, \pm 2, \cdots,$$

where σ is the interblade phase and v is an arbitrary integer.

4. Detuned rotor and stator

A stator vane row is excited by the convected wakes and steady potential field of upstream rotor blades at the multiples of the rotor blade pass frequency $\omega = nN_B\Omega$ where n is the rotor harmonic, N_B is the number of rotor blades and Ω is the shaft frequency. The stator vane responds at the excitation frequency where the unsteady stator vane loading of adjacent vanes is equal in amplitude and shifted phase by the interblade phase angle in the absolute frame $\sigma_{abs} = -2\pi nN_B/N_V$ where N_V is the number of stator vanes.

A rotor is represented in the rotating frame and is excited by the potential field of downstream stator vanes at the multiples of the stator vane pass frequency $\omega = vN_V\Omega$ where v is the stator harmonic. The stator vane responds at the excitation frequency where the unsteady stator vane loading of adjacent vanes is equal in amplitude and shifted phase by the interblade phase angle $\sigma_{rel} = 2\pi vN_V/N_B$.

The tangential wave number β_{abs} is equivalent to the spatial mode order k_θ used in annular duct acoustics. Substituting expressions for the interblade phase angle and pitch spacing gives

$$\beta_{abs} = \frac{\left(-2\pi n\left(N_B/N_V\right)\right) + 2\pi v}{\left(2\pi R/N_V\right)}, \quad v = 0, \pm 1, \pm 2, \cdots,$$

where R is the radius.

Simplifying this expression gives

$$\beta_{abs} = -\frac{1}{R}(nN_B - vN_V), \quad v = 0, \pm 1, \pm 2, \cdots.$$

The term in brackets [9] is familiar as

$$k_{\theta abs} = nN_B + vN_V, \quad v = 0, \pm 1, \pm 2, \cdots,$$

where $k_{\theta abs}$ is the spatial mode order representing the number of lobes of the rotating pressure pattern, and the sign of the v index has been switched.

The tangential periodicity of a wave does not change when represented in the rotating frame, hence $\beta_{abs} = \beta_{rel}$. The positive interblade phase angle ($\sigma_{rel} = 2\pi vN_V/N_B$) indicates that the stator moves in the negative direction in the rotor reference frame, i.e. the rotor moves up relative to the stator, and the stator moves down relative to the rotor. In the rotor reference frame, the interblade phase angle $\sigma_{rel} = 2\pi vN_V/N_B$ and rotor blade pitch spacing $S = 2\pi R/N_B$ give the tangential wave number of the rotor $\beta_{rel} = (\sigma_{rel} - 2\pi n)/S$ in the rotating frame.

Some care is required to not over specify the description of the rotor and stator geometry. Specification of the stator reduced frequency k_{stator}, the absolute Mach number M_{abs}, the stator solidity c/S_{stator}, the rotor blade to stator vane ratio N_B/N_V, the rotor chord to stator chord ratio c_B/c_V, the stagger angle of the rotor γ_{rotor}, and the stagger angle of the stator γ_{stator} fixes the

relative Mach number M_{rel}, the reduced frequency of the rotor k_{rotor}, and the solidity of the rotor c/S_{rotor}:

$$M_{rel} = M_{abs}\frac{\cos\gamma_{stator}}{\cos\gamma_{rotor}}, \quad k_{rotor} = k_{stator}\frac{N_V}{N_B}\frac{c_B}{c_V}\frac{M_{rel}}{M_{abs}}, \quad \frac{c}{S_{rotor}} = \frac{c}{S_{stator}}\frac{c_B}{c_V}\frac{N_B}{N_V}.$$

The detuned cascade spacing ratio S_r, chord ratio C_r and chordwise offset os can be specified independently for both the rotor and the stator.

Characterization of the rotor and stator unsteady aerodynamic and acoustic fields is the basis of the coupled cascade theory. Response of one cascade represents an excitation to the other. Now that the basic unsteady aerodynamics has been introduced and the geometry of the detuned rotor and stator has been defined, the solution method and the physics of cascade coupling will be explored.

5. Solution method

The unknown vortex distributions Γ on Cascades A and B are found by solving the upwash integral equation in a manner analogous to the classical tuned cascade solution. The integral is evaluated numerically using the trapezoidal rule, and a variable transformation is used to resolve the high gradients near the leading edge. This yields a linear system of equations with the upwash specified and the vortex strength unknown. A polynomial curve fit that implicitly satisfies the Kutta condition is determined to approximate the vortex strength

$$\Gamma(z_{oj}) = \sqrt{\frac{1-z_{oj}}{z_{oj}}}\sum_{\ell=0}^{n-1}\delta_\ell z_{oj}^{\ell},$$

where $z_{oj} = \frac{1}{2}(1-\cos\theta_j)$ and $\theta_j = \pi j/n$ for $j = 0, 1, \ldots, n$.

The vortex curve fit coefficients δ are determined by solution of the linear system of equations

$$\begin{bmatrix} W_A \\ W_B \end{bmatrix} = \begin{bmatrix} C_{AA} & C_{BA} \\ C_{AB} & C_{BB} \end{bmatrix}\begin{bmatrix} \delta_A \\ \delta_B \end{bmatrix},$$

where W_A and W_B are the specified upwash distributions, C_{AA}, C_{BA}, C_{AB} and C_{BB} are the components of the coefficient matrix, and δ_A and δ_B are the vortex curve fit coefficients. The curve fit coefficients are used to calculate the unsteady load on Cascade A airfoils Γ_A and the cascade B airfoils Γ_B.

5.1. Convected vortical gust upwash

To solve the upwash integral equation, the upwash is specified to satisfy the flow tangency condition on the airfoil surface. Two upwash conditions are considered: the acoustic wave upwash and the convected vortical gust upwash.

The relationship between the free vorticity ξ and the velocity is determined by the curl of the velocity,

$$\xi = \mathrm{i}(\alpha_3 v - \beta u).$$

The continuity equation $\alpha_3 u = -\beta v$ is used to relate the axial and tangential velocity components,

$$v = -\mathrm{i}\left(\frac{\alpha_3}{\alpha_3^2 + \beta^2}\right)\xi.$$

The component of velocity normal to the airfoil chord is the upwash and is related to the axial and tangential velocity components by $w = v\cos\gamma - u\sin\gamma$. Thus, the velocity induced by the gust is expressed as

$$w = -\frac{\mathrm{i}(\alpha_3\cos\gamma + \beta\sin\gamma)}{\alpha_3^2 + \beta^2}.$$

For free vorticity of unit amplitude, the upwash distribution on the cascade is

$$\frac{w_g}{W} = \frac{\mathrm{i}(\alpha_3\cos\gamma + \beta\sin\gamma)}{\alpha_3^2 + \beta^2}\exp(-\mathrm{i}kz),$$

where w_g/W is the nondimensional upwash due to a vortical gust and the $\exp(-\mathrm{i}kz)$ describes the phase change of the upwash as the gust convects along the airfoil. A negative sign has been included so that the specified amplitude of the upwash is equal and opposite that of a unit amplitude vortical disturbance.

A phase shift of the vortical gust excitation from the leading edge of Cascade A to Cascade B must be included to correctly describe the gust excitation. This phase shift is given by $\exp[\mathrm{i}(\alpha_3\Delta x_{LE} + \beta\Delta y_{LE})]$, where $(\Delta x_{LE}, \Delta y_{LE})$ is the distance from the leading edge of Cascade B to Cascade A. Thus, the upwash is

$$W_{A3} = \frac{\mathrm{i}(\alpha_3\cos\gamma + \beta\sin\gamma)}{\alpha_3^2 + \beta^2}\exp(-\mathrm{i}kz),$$

$$W_{B3} = W_{A3}\exp[\mathrm{i}(\alpha_3\Delta x_{LE} + \beta\Delta y_{LE})],$$

where W_{A3} is the upwash on Cascade A and W_{B3} has been phase shifted to Cascade B leading edge.

5.2. Acoustic wave upwash

Acoustic waves induce a velocity disturbance to the cascade. The generated unsteady velocity field imposed on the cascade is the source of the unsteady cascade loading. The tangential momentum equation relates the velocity disturbance to the amplitude of the acoustic wave.

An acoustic wave is irrotational so, $\beta u_{1,2} = \alpha_{1,2} v_{1,2}$. The axial and tangential velocity components are used to determine the upwash.

$$w_{p1,2} = -\frac{\beta\cos\gamma - \alpha_{1,2}\sin\gamma}{k + \alpha_{1,2}\cos\gamma + \beta\sin\gamma}\,\frac{P_{1,2}}{\rho_\infty W},$$

where $w_{p1,2}$ is the upwash generated by upstream and downstream going acoustic waves.

For a unit amplitude disturbance, the upwash distribution along the chord induced by a downstream going acoustic wave is

$$\frac{w_{p2}}{W} = \frac{\beta\cos\gamma - \alpha_2\sin\gamma}{k + \alpha_2\cos\gamma + \beta\sin\gamma}\exp[\mathrm{i}(\alpha_2\cos\gamma + \beta\sin\gamma)z],$$

where the upwash is referenced to the cascade leading edge.

The upstream going acoustic wave upwash is referenced to the trailing edge, so

$$\frac{w_{p1}}{W} = \frac{\beta\cos\gamma - \alpha_1\sin\gamma}{k + \alpha_1\cos\gamma + \beta\sin\gamma}\exp[\mathrm{i}(\alpha_1\cos\gamma + \beta\sin\gamma)(z-1)].$$

As in the convected vortical gust upwash, the upwash must be phase shifted to the trailing and leading edges of Cascade B for the respective upstream and downstream going acoustic wave upwash. Thus

$$\begin{aligned}
W_{A2} &= \frac{\beta\cos\gamma - \alpha_2\sin\gamma}{k + \alpha_2\cos\gamma + \beta\sin\gamma}\exp[\mathrm{i}(\alpha_2\cos\gamma + \beta\sin\gamma)z],\\
W_{B2} &= W_{A2}\exp[\mathrm{i}(\alpha_2\Delta x_{LE} + \beta\Delta y_{LE})],\\
W_{A1} &= \frac{\beta\cos\gamma - \alpha_1\sin\gamma}{k + \alpha_1\cos\gamma + \beta\sin\gamma}\exp[\mathrm{i}(\alpha_1\cos\gamma + \beta\sin\gamma)(z-1)],\\
W_{B1} &= W_{A1}\exp[\mathrm{i}(\alpha_1\Delta x_{TE} + \beta\Delta y_{TE})],
\end{aligned}$$

where $W_{A1,2}$ is the upwash due to an acoustic wave of unit amplitude and $W_{B1,2}$ has been phase shifted to the trailing and leading edges of Cascade B, respectively.

6. Far-field acoustic response

With the δ vortex curve fit coefficients determined for the specified upwash condition, the vortex distributions are calculated and the acoustic response is given by

$$P_1 = -\frac{c}{S}v_1'\int_0^1 \Gamma(z)\exp\{-\mathrm{i}(\alpha_1\cos\gamma + \beta\sin\gamma)z\}\mathrm{d}z,$$

$$P_2 = -\frac{c}{S}v_2'\int_0^1 \Gamma(z)\exp\{\mathrm{i}[1 - (\alpha_2\cos\gamma + \beta\sin\gamma)z]\}\ \mathrm{d}z,$$

where P_1 the upstream going acoustic wave is referenced to the cascade leading edge and P_2 the downstream going acoustic wave is referenced to the cascade trailing edge.

The combined acoustic response is determined by combining the individual upstream going components P_{A1} and P_{B1}, where P_{B1} must be shifted in phase from the leading edge of Cascade B to Cascade A by $\exp[\mathrm{i}(\alpha_1\Delta x_{LE} - \beta\Delta y_{LE})]$. Thus,

$$P_1 = P_{A1} + P_{B1}\exp[\mathrm{i}(\alpha_1\Delta x_{LE} - \beta\Delta y_{LE})].$$

Likewise the combined downstream going acoustic wave is phase shifted from the trailing edge,

$$P_2 = P_{A2} + P_{B2}\exp[\mathrm{i}(-\alpha_2\Delta x_{TE} - \beta\Delta y_{TE})],$$

where the components P_{A2} and P_{B2} create the combined downstream going acoustic wave P_2 and the response of Cascade B is phase shifted to the Cascade A trailing edge.

6.1. Shed wake response

The unsteady shed wake from a cascade is the integrated effect of the cascade unsteady loading,

$$\xi = -\frac{c}{S}\frac{ik}{\cos\gamma}\int_0^1 \Gamma(z)\exp\{ikz\}dz.$$

The combined shed wake response is determined by combining the individual components ξ_A and ξ_B. The combined shed wake response is phase shifted from the trailing edge,

$$\xi = \xi_A + \xi_B\exp[i(-\alpha_3\Delta x_{TE} - \beta\Delta y_{TE})],$$

where the components ξ_A and ξ_B create the combined shed wake ξ and the response of Cascade B is phase shifted to the Cascade A trailing edge.

The combined response accounts for the phase shift in the upwash and reference location, and it is the combined response that forms the basis for the cascade coupling theory. The response of one cascade represents an excitation to the other and visa versa.

7. Coupled cascade theory

A turbomachine airfoil row is excited by the potential fields of upstream and downstream airfoil rows and the convected vortical gusts of upstream airfoil rows. The unsteady velocity perturbation imposed at the solid airfoil surface produces an unsteady airfoil surface pressure required to satisfy the flow tangency condition. The unsteady airfoil loading then couples with the duct to produce a convected vortical wake and upstream and downstream going acoustic waves. In this manner, disturbances from upstream and downstream airfoil rows are transmitted and reflected by adjacent blade rows. The transmitted and reflected waves are now additional disturbances that excite the adjacent airfoil rows including the original airfoil row. The reflected and transmitted waves are not considered in a traditional isolated airfoil row analysis and can have a profound influence on the unsteady response.

Consider a rotor and stator in a duct. An upstream going acoustic wave $P_{1S}(n, v)$ from the stator is characterized by a rotor harmonic n and stator mode index v. The upstream going acoustic wave is composed of the steady stator field P_{1SX} and the upstream going pressure waves reflected from the rotor downstream going acoustic wave $S_{12}P_{2R}$ and the rotor convected vortical gust $S_{13}\xi_{3R}$,

$$P_{1S}(n,v) = P_{1SX}(n,v) + \sum_{v'} S_{12}(n,v;n,v')P_{2R} + \sum_{v'} S_{13}(n,v;n,v')\xi_{3R},$$

where S_{12} and S_{13} are the scattering coefficients.

The scattering coefficients represent the response of the stator (for S_{12} and S_{13}) to a disturbance (either P_{2R} or ξ_{3R}) of unit amplitude. Note that all rotor waves with rotor harmonic $n = n'$ and any stator mode index v' scatter into the $P_{1S}(n, v)$ upstream going pressure wave from the stator.

Also, the source terms P_{1SX}, P_{2SX} and ξ_{3SX} are non-zero only for $n = 0$, that is the stator steady field is nonzero only at zero frequency.

The downstream going acoustic wave and convected gust from the stator are given by

$$P_{2S}(n,v) = P_{2SX}(n,v) + \sum_{v'} S_{22}(n,v;n,v')P_{2R} + \sum_{v'} S_{23}(n,v;n,v')\xi_{3R},$$

where S_{22} and S_{23} scatter rotor downstream going acoustic P_{2R} and vorticity waves ξ_{3R} into stator downstream going acoustic waves P_{2S}, and

$$\xi_{3S}(n,v) = \xi_{3SX}(n,v) + \sum_{v'} S_{32}(n,v;n,v')P_{2R} + \sum_{v'} S_{33}(n,v;n,v')\xi_{3R},$$

where S_{32} and S_{33} scatter rotor downstream going acoustic P_{2R} and vorticity waves ξ_{3R} into stator vorticity waves ξ_{3S}.

The set of convected vortical gust and upstream and downstream going acoustic waves from the rotor (P_{1R}, P_{2R} and ξ_{3R}) will be composed of the steady rotor field (P_{1RX}, P_{2RX} and ξ_{3RX}) and the scattered waves ($S_{11}P_{1S}, S_{21}P_{1S}$ and $S_{31}P_{1S}$) created by the stator upstream going pressure wave. Specifically,

$$\begin{aligned}
P_{1R}(n,v) &= P_{1RX}(n,v) + \textstyle\sum_{n'} S_{11}(n,v;n',v)P_{1S}(n',v),\\
P_{2R}(n,v) &= P_{2RX}(n,v) + \textstyle\sum_{n'} S_{21}(n,v;n',v)P_{1S}(n',v),\\
\xi_{3R}(n,v) &= \xi_{3RX}(n,v) + \textstyle\sum_{n'} S_{31}(n,v;n',v)P_{1S}(n',v),
\end{aligned}$$

where S_{11}, S_{12} and S_{13} scatter the stator upstream going acoustic wave P_{1S} into stator acoustic and vorticity waves P_{1R}, P_{2R} and ξ_{3R}.

The coupling equations can be rewritten in matrix form,

$$\begin{bmatrix} I & 0 & 0 & -S_{11} & 0 & 0 \\ 0 & I & 0 & -S_{21} & 0 & 0 \\ 0 & 0 & I & -S_{31} & 0 & 0 \\ 0 & -S_{12} & -S_{13} & I & 0 & 0 \\ 0 & -S_{22} & -S_{23} & 0 & I & 0 \\ 0 & -S_{32} & -S_{33} & 0 & 0 & I \end{bmatrix} \begin{bmatrix} P_{1R} \\ P_{2R} \\ \xi_{3R} \\ P_{1S} \\ P_{2S} \\ \xi_{3S} \end{bmatrix} = \begin{bmatrix} P_{1RX} \\ P_{2RX} \\ \xi_{3RX} \\ P_{1SX} \\ P_{2SX} \\ \xi_{3SX} \end{bmatrix},$$

where the source vector is prescribed and the solution is determined through standard matrix decomposition techniques.

In summary, classical methods represent the rotor and stator as isolated airfoil rows. However, in reality, the unsteady stage response is represented by the simultaneous response and excitation caused by the steady vortical and potential fields. The coupling is accomplished through the reflection and transmission of acoustic and vorticity waves in the stage where the scattering coefficients are determined by the response to unit amplitude disturbances.

8. Sound pressure level

The acoustic response of the rotor–stator interaction is often expressed either in terms of the sound pressure level or the intensity level. The sound pressure level is defined as $SPL = 20\log_{10}(P/P_{ref})$ where P is the amplitude of a propagating acoustic wave and amplitude of the reference pressure P_{ref} is 4.1×10^{-9} psi.

The propagating modes generated by the cascades are spatially periodic and exist at multiples of the rotor blade pass frequency (in the absolute frame). At any given instant in time, The acoustic waves will constructively/destructively interfere at different locations around the annulus, but the amount of energy in each of these propagating acoustic waves is proportional to the square of the pressure. Overall the total amount of propagating acoustic energy is proportional to the sum of each of the individual propagating waves. Thus, the overall sound pressure level is given by

$$SPL = 20\log_{10}\left(\frac{\sum}{P_{ref}}\right)$$

where $\sum P$ is total amplitude of the propagating acoustic waves over all harmonics and spatial modes. Thus, the overall sound pressure level is the best measure of noise generation to compare the acoustic response of tuned and detuned stages at each operating condition.

9. Results

A classical analysis considers a rotor and stator in isolation, i.e. the rotor configuration has no bearing on the acoustic response of the stator and visa versa. Using a coupled analysis, the endeavor is to reduce the overall acoustic response of the stage comprised of a rotor and stator row and quantify the influence of the detuned stage configuration.

The influence of aerodynamic detuning on the discrete-frequency acoustic response of a turbomachinery stage is determined by applying the model described herein to a tuned stage with 18 rotor blades and 38 stator vanes. At blade pass frequency, this design is "cut-off" and no propagating acoustic waves are generated for subsonic rotor relative Mach numbers. The tuned stator row has a pitch spacing of one chord and zero stagger. The stage is defined by the rotor–stator chord ratio of 0.474 (the rotor and stator have a pitch spacing of 1 chord). For a machine with a radius of 3 ft spinning at 2820 rpm, the reduced frequency at blade pass frequency is 6.0. The rotor and stator are staggered at -63.6° and 0°, respectively. The axial spacing of the cascades Δx is equal to one quarter of the stator chord. An absolute Mach number of 0.4 gives a rotor relative Mach number of 0.9. Propagation of acoustic waves begins at an absolute Mach number of 0.08. Thus, the acoustic response upstream of the rotor and downstream of the stator is determined in the range of absolute Mach numbers from 0.08 to 0.4.

For the coupled analysis of the baseline tuned stage configuration, the tuned cascade is characterized as a detuned stage with 9 rotor blades and 19 stator vanes, i.e., Cascades A and B representation have one-half the number of airfoils of the tuned cascade configuration, Fig. 2. The baseline detuned stage geometry has a rotor and stator having a chord ratio of 0.5, a spacing ratio of 0.5 and zero chordwise offset, Fig. 3. Because the detuned rotor has 9 full chord and 9 splitter

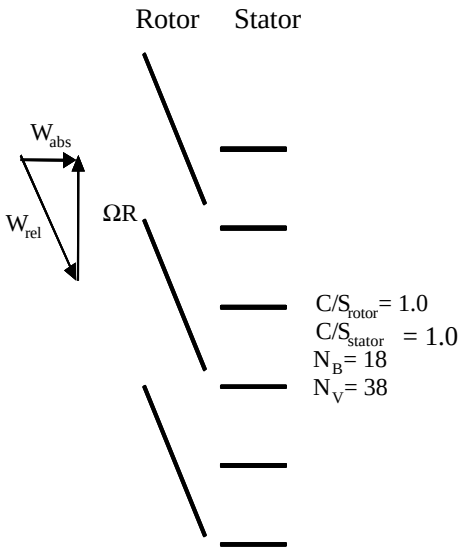

Fig. 2. Baseline tuned geometry.

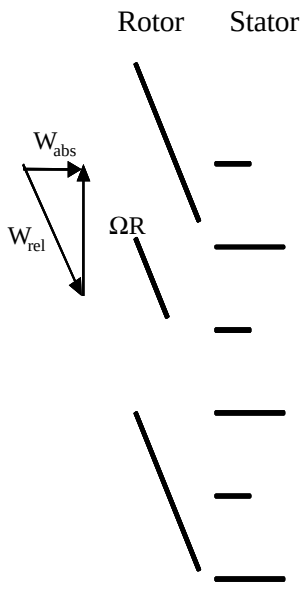

Fig. 3. Baseline detuned geometry. Rotor: $C_r = 0.5$, $S_r = 0.5$, $os = 0.0$. Stator: $C_r = 0.5$, $S_r = 0.5$, $os = 0.0$.

blades, the reduced frequency drops from 6.0 from the tuned cascade to 3.0 for the first rotor harmonic.

The coupled cascade analysis is achieved by selecting a certain number of modes to include in the mode-coupling scheme. The rotor steady field is characterized by modes $(n, v) =$

$\{(1,0),(2,0),(3,0),(4,0),(5,0),(6,0)\}$. These modes rotate with the rotor and have tangential periodicity given by a multiple of the number of rotor blades $\beta = -1/R(nN_{\mathbf{B}})$. Likewise, the stator steady field is given by modes $(n,v) = \{(0,1),(0,2),(0,3),(0,4),(0,5),(0,6)\}$. These modes are steady in the absolute frame and rotate with the stator in the rotating frame. The steady stator field modes have tangential periodicity given by multiples of the number of stator vanes $\beta = -1/R(\mathrm{v}N_V)$. The acoustic waves generated by the rotor–stator interaction yield propagating acoustic waves where $(n,v) = \{(2,1),(3,1),(4,2),(5,2),(5,3),(6,2),(6,3)\}$.

By way of example, consider the $(n,v) = (4,2)$ acoustic wave. Using $k_\theta = nN_B - vN_V$, the $(n,v) = (4,2)$ acoustic wave corresponds to a two-lobed spatial mode $k_\theta = -2$ generated at fourth harmonic of the detuned rotor. The negative sign of the wave number indicates that acoustic wave spins in the opposite direction of the rotor rotation.

The endeavor is to determine a detuned rotor and stator geometry that minimizes the combined acoustic response of the propagating interaction modes. By symmetry, superposition of the "odd" harmonic ($n = 1,3,5$ or $v = 1,3,5$) for a tuned cascade gives unsteady loading and acoustic response that is identically zero. That is the response of Cascade A is equal and opposite of the response of Cascade B. Thus, the acoustic waves given by $(n,v) = \{(2,1),(3,1),(5,2),(5,3),(6,3)\}$ exist only for the detuned cascades, while the acoustic waves given by $(n,v) = \{(4,2),(6,2)\}$ exist for both the tuned and detuned cascades.

The coupled cascade theory and unsteady aerodynamic analysis do not provide the amplitude of the steady potential fields or the amplitude of the shed vortical wake of the rotor and the stator. The following model is utilized where the amplitude of the detuned pressure and vorticity fields are phase shifted using the spacing ratio. The vortical and potential excitation of the rotor $_{3\mathrm{RX}}$ and $\mathrm{P}_{2\mathrm{RX}}$ and the potential excitation of the stator $\mathrm{P}_{1\mathrm{SX}}$ are determined by superposition dependent on the spacing ratio only:

$$P_{1SX} = \bar{P}_{1SX}(1 + \exp\{\mathrm{i}(2S_r)\pi v\}),$$
$$P_{2RX} = \bar{P}_{2RX}(1 + \exp\{\mathrm{i}(2S_r)\pi n\}),$$
$$\xi_{3RX} = \bar{\xi}_{3RX}(1 + \exp\{\mathrm{i}(2S_r)\pi n\}),$$

where $\bar{P}_{1SX}, \bar{P}_{2RX}$ and $\bar{\xi}_{3RX}$ represent the amplitude of the steady disturbance. The amplitudes in Table 1 give the non-dimensional amplitude of the vortical and potential waves as a function of rotor or stator harmonic. These amplitudes are representative of the unsteady flow field generated by high-speed axial flow turbomachines. For example, the upwash generated at the second rotor harmonic by the convected vortical gust ξ_{3RX} represents an upwash velocity of 5% of the freestream velocity, and the acoustic perturbation generated by the rotor steady field is 25% of the dynamic pressure $\rho_\infty W^2$.

When the spacing ratio is 0.5 (as it is in a tuned cascade), the odd terms cancel identically. Thus, this model matches the minimum tuned cascade periodicity requirements. This model for the steady excitation is an approximation that does not include the change in the steady field due to changes in the chord ratio, but it does retain the most basic symmetry requirements for a tuned cascade. That is, when $S_r = 0.5$ and n is odd the excitation is zero, and when $S_r = 0.5$ and n even the excitation is non-zero.

For an uncoupled rotor, the second harmonic of the stator potential field $P_{1SX}(0,2)$ generates two propagating acoustic waves $P_{1R}(4,2)$ and $P_{1R}(6,2)$ where the amplitude of the response is

Table 1
Steady excitation amplitudes

Harmonic	$\bar{P}_{2RX}$	$\bar{\xi}_{3RX}$	$\bar{P}_{1SX}$
1	0.25	0.2	0.125
2	0.25	0.2	0.125
3	0.125	0.18	0.063
4	0.125	0.18	0.063
5	0.063	0.15	0.031
6	0.063	0.15	0.031

determined using the scattering coefficients $S_{11}(4,2;0,2)$ and $S_{11}(6,2;0,2)$:

$$P_{1R}(4,2) = S_{11}(4,2;0,2)P_{1SX}(0,2), P_{1R}(6,2) = S_{11}(6,2;0,2)P_{1SX}(0,2)$$

Likewise, the downstream propagating acoustic response of the uncoupled rotor is given by

$$P_{2R}(4,2) = S_{21}(4,2;0,2)P_{1SX}(0,2), P_{2R}(6,2) = S_{21}(6,2;0,2)P_{1SX}(0,2),$$

where the downstream propagating acoustic waves $P_{2R}(4,2)$ and $P_{2R}(6,2)$ are generated by the stator potential field $P_{1SX}(0,2)$.

The acoustic waves propagating upstream from the uncoupled stator $P_{1S}(4,2)$ and $P_{1S}(6,2)$ are excited by both the steady potential field of the rotor $P_{2RX}(4,0)$ and $P_{2RX}(6,0)$. The amplitude are

$$P_{1S}(4,2) = S_{12}(4,2;4,0)P_{2RX}(4,0) + S_{13}(4,2;4,0)\xi_{3RX}(4,0),$$
$$P_{1S}(6,2) = S_{12}(6,2;6,0)P_{2RX}(6,0) + S_{13}(6,2;6,0)\xi_{3RX}(6,0).$$

For an uncoupled analysis, the amplitudes of the propagating acoustic waves from the rotor and the stator are simply summed

$$P_1(4,2) = Amp(P_{1S}(4,2)) + Amp(P_{1R}(4,2)), P_1(6,2) = Amp(P_{1S}(6,2)) + Amp(P_{1R}(6,2)),$$

$$P_2(4,2) = Amp(P_{2S}(4,2)) + Amp(P_{2R}(4,2)), P_2(6,2) = Amp(P_{2S}(6,2)) + Amp(P_{2R}(6,2)),$$

where P_1 and P_2 are the amplitudes of the upstream and downstream propagating acoustic waves from the uncoupled stage.

While the overall acoustic response of the uncoupled cascade is given by P_1 and P_2 as determined above, the acoustic response of the coupled stage is given by P_{1R} and P_{2S}. The acoustic waves propagating downstream from the rotor P_{2R} and upstream from the stator P_{1S} are internal to the stage and do not "escape". The influence of cascade coupling is determined by comparing the overall acoustic response, i.e. the sum of the propagating mode amplitudes. The neglect of cascade coupling has a drastic effect on the acoustic response of the stage, with the upstream response significantly over predicted and the downstream acoustic response significantly under predicted and errors as high as 20 dB for certain operating conditions, Figs. 4 and 5.

Figs. 6–9 show the coupled cascade response of the baseline tuned and detuned cascades in detail. Upstream, the fourth harmonic dominates the overall acoustic response of the tuned cascade, but downstream the individual modes have comparable amplitude. Recall, the baseline-

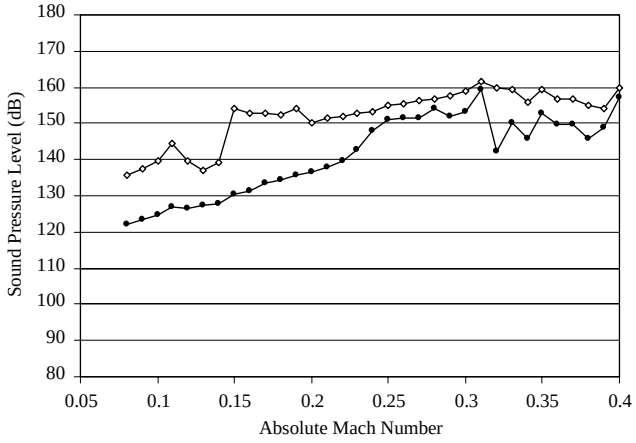

Fig. 4. Cascade coupling influence on upstream acoustic response: —●—, coupled; —◇—, uncoupled.

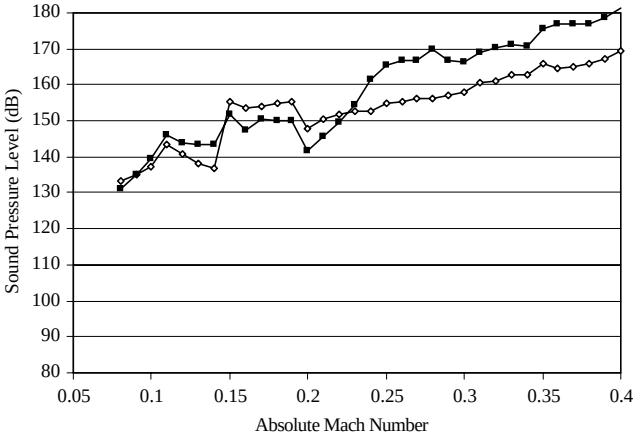

Fig. 5. Cascade coupling influence on downstream acoustic response: —●—, coupled; —◇—, uncoupled.

detuned stage has rotor and stator chord ratios of 0.5, rotor and stator spacing ratios of 0.5 and rotor and stator chordwise offsets of 0.0. Thus, the baseline-detuned stage has alternate airfoils replaced with 50% chord splitters with all other rotor and stator parameters unchanged. Detuning of the baseline-tuned stage generates a multitude of "odd" $(n, v) = \{(2,1),(3,1),(5,2),(5,3),(6,3)\}$ propagating modes in addition to the "even" $(n, v) = \{(4,2),(6,2)\}$ modes where individual "even" mode amplitudes are reduced. The reduction in the "even" propagating wave amplitudes is mitigated by the generation of the "odd" propagating waves of the detuned stage.

Given the increased number of propagating acoustic waves, it is easy to understand why the overall acoustic response of the stage is the appropriate benchmark where the overall SPL is calculated using the summed amplitude of the propagating modes. A direct comparison of the tuned and detuned overall acoustic response is given in Fig. 10 and 11. The detuning of the stage is seen to be beneficial over most of the operating range.

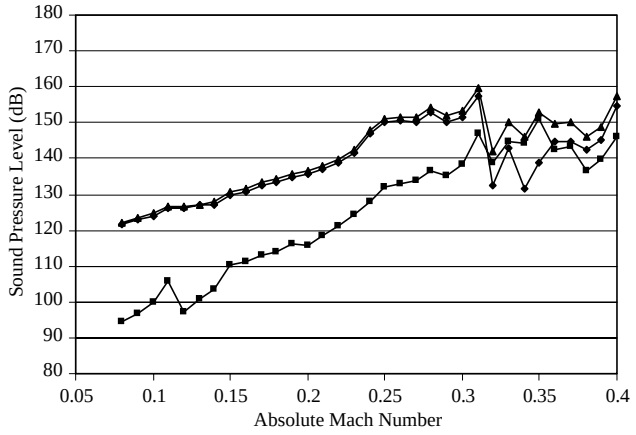

Fig. 6. Upstream acoustic response of the coupled tuned cascade: —◆—, (4,2); —■—, (6,2); —▲—, overall.

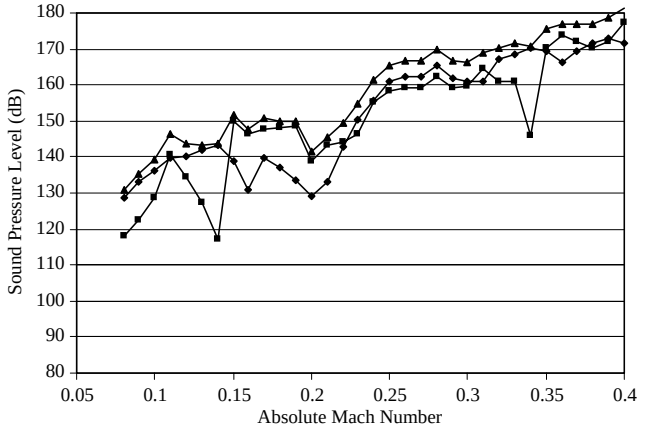

Fig. 7. Downstream acoustic response of the coupled tuned cascade: —◆—, (4,2); —■—, (6,2); —▲—, overall.

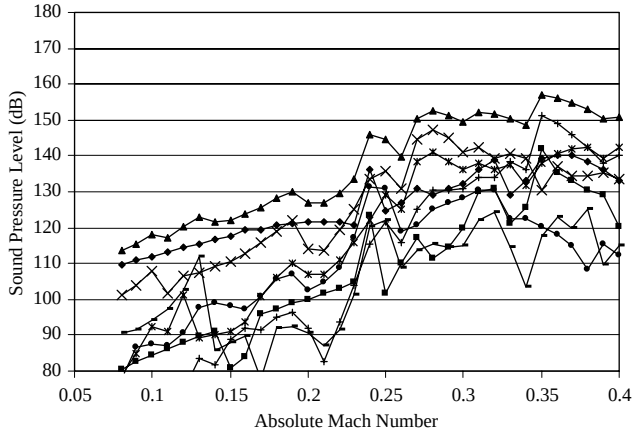

Fig. 8. Upstream acoustic response of the coupled detuned cascade: —×—, (4,2); —✳—, (5,2); —×—, (4,2); —✳—, (5,2); —●—, (5,3); —+—, (6,2); —●—, (5,3); —+—, (6,2).

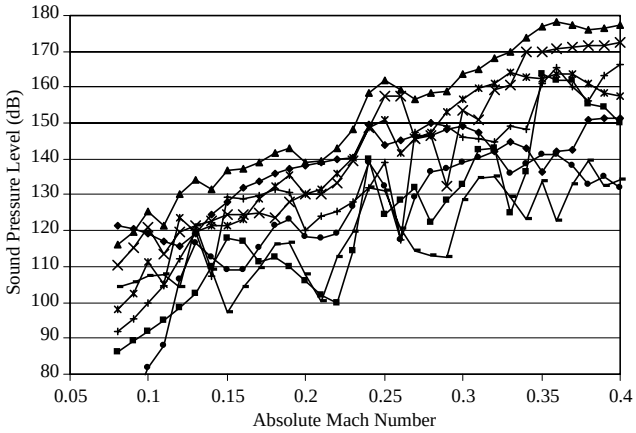

Fig. 9. Downstream acoustic response of the coupled detuned cascade: —×—, (4,2); —✳—, (5,2); —×—, (4,2); —✳—, (5,2): —●—, (5,3); —+—, (6,2); —●—, (5,3); —+—, (6,3).

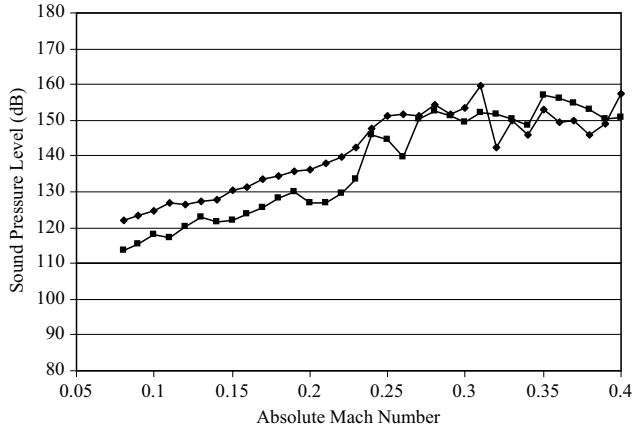

Fig. 10. Overall upstream acoustic response of the tuned and detuned coupled cascades: —◆—, tuned; —■—, detuned.

The question remains if the baseline detuned stage geometry can be optimized to significantly decrease the stage acoustic response. Thus, the chord ratio, spacing ratio and chordwise offset are varied individually at the 0.2 absolute Mach number condition to determine the optimum detuned stage configuration. The response of this configuration will then be determined over the operating range of absolute Mach numbers from 0.08 to 0.4.

The influence of rotor and stator chord ratio is determined in Fig. 12. The combined overall upstream and downstream acoustic response is calculated to determine the optimum chord ratio. The combined overall acoustic response is defined by the sum of all upstream and downstream propagating acoustic waves.

The stage acoustic response is determined as a function of rotor chord ratio while the stator chord ratio is constant and a function of the stator chord ratio while the rotor chord ratio is held

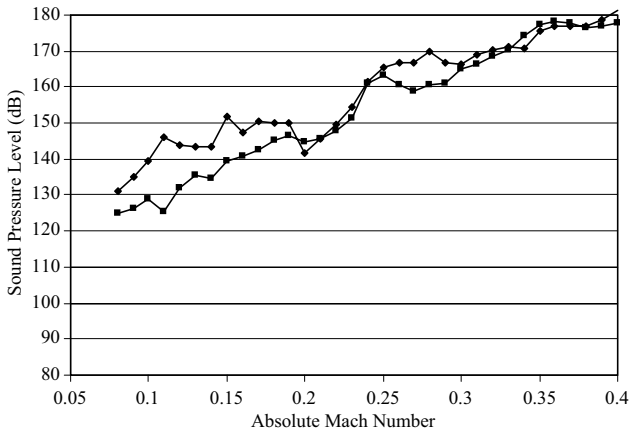

Fig. 11. Overall downstream acoustic response of the tuned and detuned coupled cascades: —◆—, tuned; —■—, detuned.

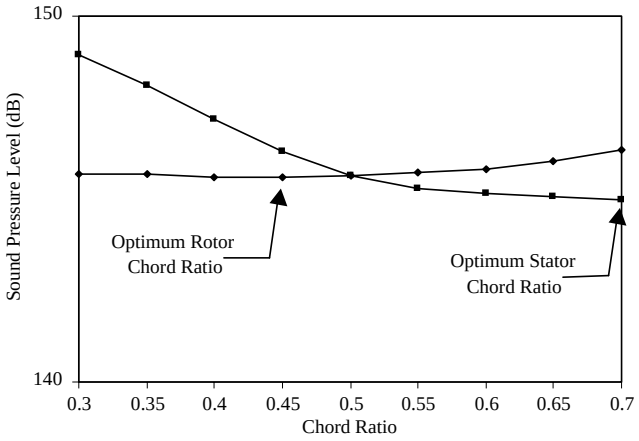

Fig. 12. Chord ratio influence on combined acoustic response of the detuned coupled cascades: —◆—, rotor; —■—, stator.

constant. One may initially suspect that a reduced splitter chord corresponds to reduced acoustic response, but this is not the case as the optimum rotor and stator chord ratios are 0.45 and 0.7, respectively. The combined upstream and downstream acoustic response is a relatively weak function of the rotor chord ratio.

There is no clear trend in the spacing ratio influence on the stage acoustic response. This is shown in Fig. 13 where the acoustic response is determined as a function of rotor spacing ratio while the stator spacing ratio is constant and a function of the stator spacing ratio while the rotor spacing ratio is held constant. The optimum rotor and stator spacing ratios are 0.7 and 0.5 based on the combined upstream and downstream acoustic response.

Fig. 14 shows that the chordwise offset of the rotor's 45% chord splitter blades has only a very small effect on the combined upstream and downstream acoustic response of the stage. For the rotor, the chordwise offset is varied from zero where the leading edge of the full chord and splitter

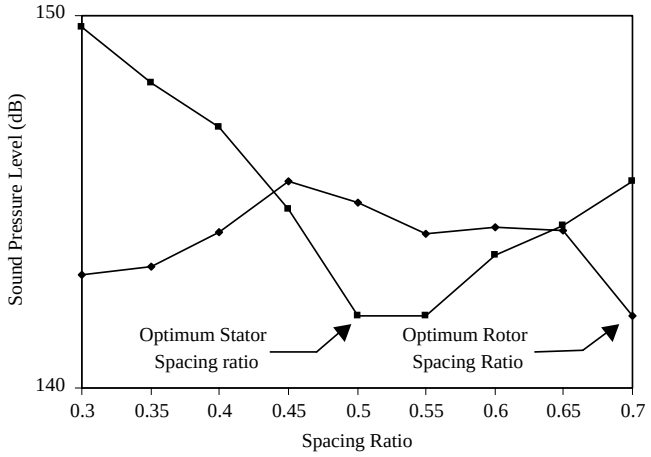

Fig. 13. Spacing ratio influence on combined acoustic response of the detuned coupled cascades: —◆—, rotor; —■—, stator.

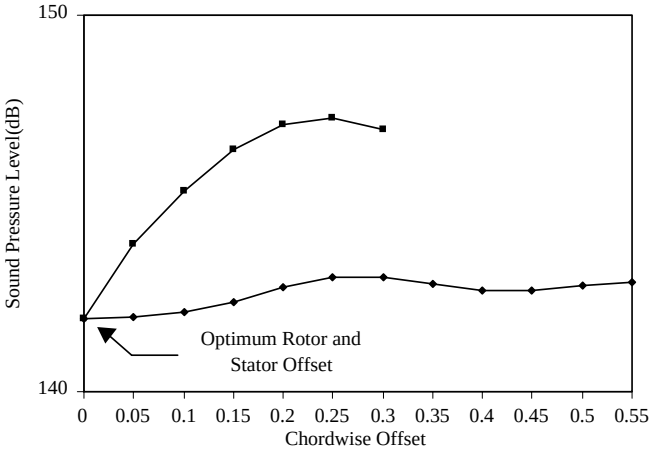

Fig. 14. Chordwise offset influence on detuned coupled cascade combined acoustic response: —◆—, rotor; —■—, stator.

blades is aligned to 0.55 where the trailing edge of the rotor's full chord and splitter blades are aligned. Likewise, the influence of stator chordwise offset of the 70% chord splitter vanes is determined from zero to 0.3 where the leading and trailing edges are aligned, respectively. The optimum combined acoustic response occurs when both the rotor and stator chordwise offset is 0.0.

The preceding figures have determined the optimum detuned stage configuration for the 0.2 absolute Mach number operating condition. The optimized rotor is configured with a chord ratio of 0.45, a spacing ratio of 0.7, and a chordwise offset of 0.0. The optimized stator configuration is 0.7-chord ratio, 0.5 spacing ratio and no chordwise offset. The geometry of the baseline and optimized detuned cascades is shown in Figs. 15 and 16.

Fig. 17 shows the impact of the optimization relative to the tuned and baseline detuned stages. The optimized detuned geometry lowered the upstream going acoustic response by just less than

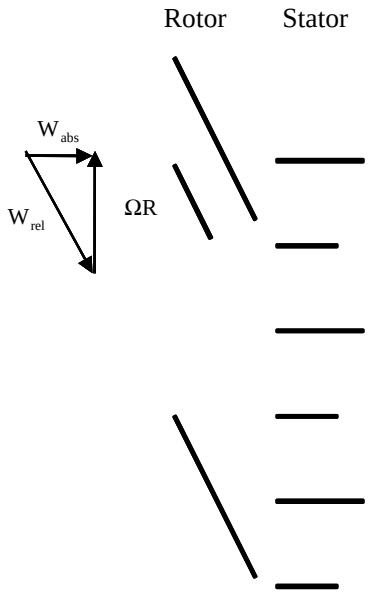

Fig. 15. Baseline detuned configuration. Rotor: $C_r = 0.75$, $S_r = 0.70$, $os = 0.0$. Stator: $C_r = 0.70$, $S_r = 0.50$, $os = 0.0$.

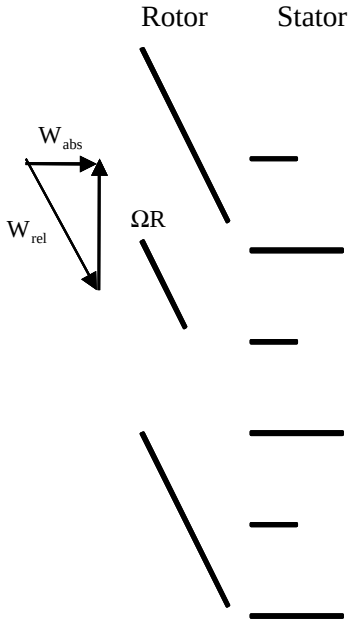

Fig. 16. Optimum detuned configuration. Rotor: $C_r = 0.50$, $S_r = 0.50$, $os = 0.0$. Stator; $C_r = 0.50$, $S_r = 0.50$, $os = 0.0$.

13 dB relative to the tuned cascade. Downstream, where the baseline detuned stage actually had higher acoustic response shows a more modest 4 dB decrease relative to the baseline detuned stage, but only 1 dB relative to the tuned stage.

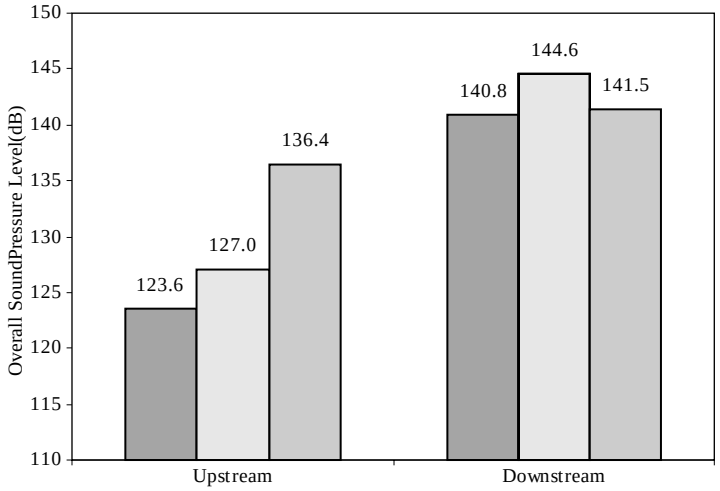

Fig. 17. Acoustic response of optimized coupled baseline detuned and tuned cascades: ■, optimum; ■, baseline; ■, tuned.

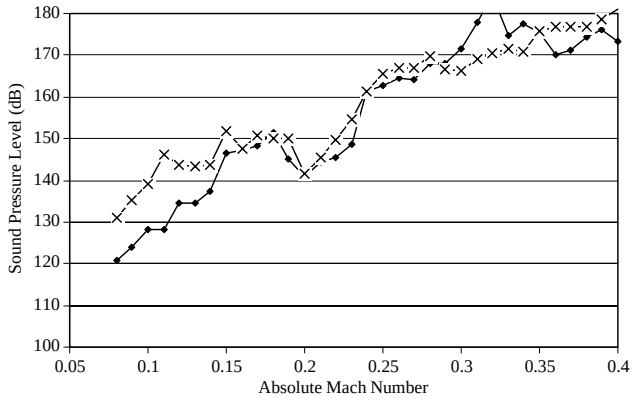

Fig. 18. Overall acoustic response of the optimum detuned and tuned cascades: —•—, optimum downstream; –×–, tuned upstream.

The upstream and downstream propagating acoustic response for the baseline tuned and the optimized detuned stages is shown in Fig. 18. Detuning is most effective at lower Mach numbers with maximum reductions of 12–15 dB relative to the tuned stage. At higher Mach numbers for this detuned geometry, detuning is less effective or even detrimental to the upstream and downstream acoustic response.

10. Summary and conclusions

An analytical model has been developed to determine the unsteady aerodynamics and subsequent acoustic response of an aerodynamically detuned turbomachinery stage. The

two-dimensional model considers a compressible flow with small unsteady pressure and velocity perturbations superimposed. The cascade model considers coupled flat-plate airfoils at zero incidence with the mean flow. The rotor–stator coupling is accomplished through the scattering of acoustic and vorticity waves between the rotor and the stator.

The overall acoustic response of a baseline tuned stage configuration was determined over a range of operating conditions utilizing the coupled unsteady aerodynamic analysis. The acoustic response of the tuned stage was compared to the response of the aerodynamically detuned stage with half–chord splitters. The optimum chord ratio, spacing ratio and chordwise offset were then determined for both the rotor and the stator at a single operating condition. This optimized stage configuration achieved noise reductions of 13 and 1 dB upstream and downstream at the design operating condition. The relative noise reduction was then determined over the range of operating conditions, with reductions on the order of 5–10 dB over the low Mach number operating conditions.

Acknowledgements

This research was sponsored by the NASA Glenn Research Center and the Air Force Office of Scientific Research (AFOSR). This support is most gratefully acknowledged.

Appendix A. Nomenclature

A	cascade A airfoil index
B	cascade B airfoil index
C_A	chord length of Cascade A
C_B	chord length of Cascade B
C_r	ratio of chord length of Cascade B to Cascade A
k	reduced frequency $k = \omega c/W$
n	rotor harmonic
N_B	number of rotor blades
os	chordwise offset of Cascade B to Cascade A
$P_{1,2}$	up- and down-stream going pressure waves
$\bar{p}$	complex pressure perturbation strength
S	circumferential spacing
S_{ij}	scattering coefficient where $i,j = 1, 2$ or 3
S_o	circumferential distance between adjacent Cascades A and B airfoils
S_r	circumferential spacing ratio $S_r = S_o/S$
u	unsteady axial velocity perturbation
$\bar{u}$	axial velocity perturbation strength
U	freestream axial velocity
v	stator vane index
v	unsteady tangential velocity perturbation
$\bar{v}$	tangential velocity perturbation strength

V freestream tangential velocity
w upwash normal to the airfoil
W freestream flow velocity
x axial co-ordinate
y tangential co-ordinate
z chordwise co-ordinate
ρ unsteady density perturbation
ρ_∞ freestream density
α axial wave number
β tangential wave number
Γ bound vortex distribution
γ stagger angle
σ interblade phase angle
ω excitation frequency $\omega = nN_B\Omega$
Ω rotor shaft frequency
ξ free vorticity

References

[1] P.R. Gliebe, Aeroacoustics, Turbomachines and propellers—future research needs, in: H.F. Atassi (Ed.), Unsteady Aerodynamics, Aeroacoustics, and Aeroelasticity of Turbomachines and Propellers, Springer, Berlin, pp. 619–642.
[2] J.F. Groeneweg, E.J. Rice, Aircraft turbofan noise, American Society of Mechanical Engineers Journal of Turbomachinery 109 (1987) 130–141.
[3] D.B. Hanson, Mode trapping in coupled 2D cascades—acoustic and aerodynamic results, American Institute of Aeronautics and Astronautics Paper 93-4417, 1993.
[4] D.H. Buffum, Blade row interaction effects on flutter and forced response, Journal of Propulsion and Power 11 (1995) 205–212.
[5] P.D. Silkowski, K.C. Hall, A coupled mode analysis of unsteady multistage flows in turbomachinery, Transactions of the American Institute of Aeronautics and Astronautics 120 (1988) 410–421.
[6] H.D. Chiang, S. Fleeter, Passive control of flow induced vibrations by splitter blades, American Society of Mechanical Engineers Journal of Turbomachinery 116 (1994) 489–500.
[7] S. Sawyer, S. Fleeter, Flutter stability of a detuned cascade in subsonic compressible flow, American Institute of Aeronautics and Astronautics Journal of Propulsion and Power 11 (1995) 923–930.
[8] S.N. Smith, Discrete frequency sound generation in axial flow turbomachines, ARC R & M 3709, 1972.
[9] J.M. Tyler, T.G. Sofrin, Axial flow compressor noise studies, SAE Transactions 70 (1962) 309–332.